Published in final edited form as:

Biol Blood Marrow Transplant. 2015 July ; 21(7): 1237–1245. doi:10.1016/j.bbmt.2015.03.011.

Dynamical System Modeling of Immune Reconstitution after Allogeneic Stem Cell Transplantation Identifies Patients at Risk for Adverse Outcomes

Amir A. Toor[1,*], **Roy T. Sabo**[2], **Catherine H. Roberts**[1], **Bonny L. Moore**[1], **Salman R. Salman**[1], **Allison F. Scalora**[1], **May T. Aziz**[3], **Ali S. Shubar Ali**[1], **Charles E. Hall**[1], **Jeremy Meier**[1], **Radhika M. Thorn**[1], **Elaine Wang**[1], **Shiyu Song**[4], **Kristin Miller**[5], **Kathryn Rizzo**[6], **William B. Clark**[1], **John M. McCarty**[1], **Harold M. Chung**[1], **Masoud H. Manjili**[7], and **Michael C. Neale**[8]

[1]Bone Marrow Transplant Program, Massey Cancer Center, Department of Internal Medicine, Virginia Commonwealth University, Richmond, Virginia

[2]Department of Biostatistics, Virginia Commonwealth University, Richmond, Virginia

[3]Department of Pharmacy and Therapeutics, Virginia Commonwealth University, Richmond, Virginia

[4]Department of Radiation Oncology, Virginia Commonwealth University, Richmond, Virginia

[5]Department of Internal Medicine, Virginia Commonwealth University, Richmond, Virginia

[6]Department of Pathology, Virginia Commonwealth University, Richmond, Virginia

[7]Department of Microbiology & Immunology, Virginia Commonwealth University, Richmond, Virginia

[8]Departments of Psychiatry & Human Genetics, Virginia Commonwealth University, Richmond, Virginia

Abstract

Systems that evolve over time and follow mathematical laws as they evolve are called *dynamical systems*. Lymphocyte recovery and clinical outcomes in 41 allograft recipients conditioned using antithymocyte globulin (ATG) and 4.5-Gy total body irradiation were studied to determine if immune reconstitution could be described as a dynamical system. Survival, relapse, and graft-versus-host disease (GVHD) were not significantly different in 2 cohorts of patients receiving different doses of ATG. However, donor-derived $CD3^+$ cell reconstitution was superior in the lower ATG dose cohort, and there were fewer instances of donor lymphocyte infusion (DLI). Lymphoid recovery was plotted in each individual over time and demonstrated 1 of 3 sigmoid growth patterns: Pattern A (n = 15) had rapid growth with high lymphocyte counts, pattern B (n =

[*]Correspondence and reprint requests: Amir A. Toor, MD, Associate Professor of Medicine, Massey Cancer Center, Virginia Commonwealth University, 1300 E Marshall St, PO Box 980157, Richmond, VA 23298-0157. atoor@mcvh-vcu.edu.

Conflicts of interest statement: A.A.T. has received research support from Sanofi-Aventis.

Supplementary Data: Supplementary data related to this article can be found at http://dx.doi.org/10.1016/j.bbmt.2015.03.011.

Financial disclosure: The authors gratefully acknowledge Sanofi-Aventis, the manufacturers of Thymoglobulin, for their support of this clinical trial. Dr. Neale was supported by Commonwealth Health Research Board grant no. 236-11-13.

14) had slower growth with intermediate recovery, and pattern C (n = 10) had poor lymphocyte reconstitution. There was a significant association between lymphocyte recovery patterns and both the rate of change of donor-derived $CD3^+$ at day 30 after stem cell transplantation (SCT) and clinical outcomes. GVHD was observed more frequently with pattern A, relapse and DLI more so with pattern C, with a consequent survival advantage in patients with patterns A and B. We conclude that evaluating immune reconstitution after SCT as a dynamical system may differentiate patients at risk of adverse outcomes and allow early intervention to modulate that risk.

Keywords

Stem cell transplant; Dynamical system; Immune reconstitution; T cells; Graft-versus-host disease

Introduction

Allogeneic stem cell transplantation (SCT) results in widely disparate outcomes in individual transplant recipients, regardless of uniformity of histocompatibility criteria applied in donor selection [1-3] and therapeutic interventions [4-6] used for pretransplant conditioning regimens and graft-versus-host disease (GVHD) prophylaxis. Standard methodology is to examine clinical outcomes using statistical analytic techniques based on probability theory [7,8]. These analytic techniques are useful in determining odds of clinical outcomes in populations of patients transplanted using uniform conditioning regimens but are inadequate for determining the course an individual might take after SCT. This is because of the underlying assumption that within the constraints of certain critical parameters, such as donor type or HLA matching, the probability distribution of these clinical outcomes is essentially random. As an example, the addition of antithymocyte globulin (ATG) to the conditioning regimen reduces the *likelihood* of developing severe acute GVHD [9], and higher levels of donor T cell chimerism at day 30 after reduced-intensity conditioning (RIC) results in a lower *probability* of relapse after SCT [10]. Such population-based estimates are used to guide clinical decision-making at various time points during the transplant process, but individual patients undergoing SCT remain at risk for competing causes of adverse outcomes.

To improve outcome predictions in individuals undergoing SCT in real time, a closer examination of the immunobiology of transplantation is necessary. In SCT treatment, failure is often attributable to either the development of immune-mediated GVHD or the lack of an immune graft-versus-malignancy (GVM) effect [11-16]. Donor-derived immune reconstitution is driven, in part, by the disparity in minor histocompatibility antigens encountered in each instance of SCT [17,18]. It has been demonstrated that HLA-matched donor–recipient pairs have extensive variation in their exomes [19]. When analyzed in silico, this translates to a massive array of minor histocompatibility antigens, which may be presented by the HLA in the recipients [20]. This minor histocompatibility antigen difference may be considered an alloreactivity potential between donors and recipient pairs and appears to mirror the complex T cell clonal frequency observed in the T cell repertoire in SCT donors and recipients [21]. This suggests that clinical outcomes related to T cell alloreactivity after SCT may not be primarily stochastic in nature but when taking a

quantitative perspective may be better considered mathematically to account for the large alloreactivity potential between SCT donors and recipients.

Systems that follow mathematically defined laws are common in the natural world and are called *dynamical systems* [22-25]. A dynamical system is defined as any *iterating* physical system that *evolves* over time in a manner such that *future* states of the system are predicated on *all* the *preceding states* and the evolution of the system can be modeled using ordinary differential equations. Population growth constrained by environmental pressures is a nonlinear example of such a system. In the context of SCT, this implies that if considered as a system of interacting donor T cell clones and recipient antigens, immune reconstitution after SCT is a dynamic, evolving process that can be modeled mathematically and allow more precise determination of the odds of clinical outcomes, such as engraftment, GVHD, and survival, in an individual [26]. A feature of dynamical systems is that early events in the system set the trajectory of the series of events to follow and thus determine the eventual outcome. In nonlinear dynamical systems, this implies that small variations in the early state of the system can produce large measurable effects late in the evolution of this system. In SCT a large body of literature now supports the notion that both early interventions [27-29] and the magnitude of immune reconstitution early in the course of SCT impacts late clinical outcomes [13,30,31], supporting the validity of considering SCT as a nonlinear dynamical system.

In this article the results of a prospective, randomized, phase II clinical trial are reported and considered in the light of immune reconstitution kinetics modeled as a dynamical system. The trial investigated 2 doses of rabbit ATG (Thymoglobulin; Sanofi-Aventis, Quebec, Canada) in patients undergoing RIC. The trial was designed to determine the optimal dosing of ATG to be given in combination with reduced-intensity total body irradiation (TBI) to ensure adequate engraftment. The clinical outcomes from this trial are analyzed with an underlying assumption that each transplant represents an example of a dynamical system. Each donor–recipient pair is composed of a unique set of recipient alloantigens and a set of donor-derived immune effectors interacting over time after the transplant event, in this instance modulated by 2 different ATG doses. The focus of the work presented here is on total lymphoid and T cell reconstitution and the resulting clinical effect. We demonstrate that lymphoid reconstitution after transplantation follows the ubiquitous quantitative rules describing constrained growth, that is, it occurs as a logistic function of time.

Methods

Patients

Between 2009 and 2013, 41 patients were enrolled in a prospective, randomized, phase II clinical trial, approved by the institutional review board at Virginia Commonwealth University (ClinicalTrials.gov Identifier: NCT00709592). To be eligible, patients had to be ≤70 years old with recurrent or high-risk hematological malignancy. Patients were required to have a 7/8 or 8/8 locus matched related or unrelated donor, with high-resolution typing performed for HLA-A, -B, -C, and -DRB1. Two different doses of ATG were tested in the 2 arms of this trial, and patients were stratified for donor type (matched related or unrelated donor) and disease status (first complete remission or higher) at the time of randomization.

Patient characteristics are given in Table 1. Patient follow-up was updated as of October 2014.

Rabbit ATG and Low-Dose TBI Conditioning Regimen

Patients were randomized between 2 different doses of rabbit ATG, either 2.5 or 1.7 mg/kg, adjusted ideal body weight per day given intravenously from day −9 to −7 (ATG 7.5 or ATG 5.1 cohorts), followed by TBI to a total dose of 4.5 Gy, delivered in 3 1.5-Gy fractions, administered twice on day −1, with the final dose on day 0 (see Supplemental Figure 1 and Supplemental Material). Tacrolimus given orally for GVHD prophylaxis from day −2, with taper commencing around 12 weeks post-transplant, in an initial cohort of patients (n = 24) and according to donor-derived T cell counts in the remaining patients. Mycophenolate mofetil (MMF) was given orally at a dose of 15 mg/kg twice daily from days 0 to 30. Escalating-dose donor lymphocyte infusion (DLI) was permitted beyond 8 weeks post-SCT for the management of declining or persistent mixed chimerism and for disease progression.

Lymphoid Reconstitution after SCT

Absolute lymphocyte counts (ALCs, μL^{-1}), measured at multiple time points as a part of routine clinical care of the patients after SCT, were plotted over time and analyzed using GraphPad Prism version 6.00 for Windows (GraphPad Software, La Jolla, CA). These data were examined for trends over time and further analyzed as a logistic function of time using the equation of the general form, $N_t = N_0 + (K–N_0)/(1 + 10^{(a–t)R})$ (adopted from Prism version 6.00). In this equation, N_0 represents the lymphocyte count at the beginning, K is the lymphocyte count at steady state, N_t is the lymphocyte count at time t after transplant, a is the time at which growth rate is maximal and an inflection point is observed in the logistic curve, and R is the growth rate of the population. To elucidate the initial growth followed by exponential expansion of the lymphocytes and to eliminate the effect of extraneous therapy on lymphocyte counts (eg, corticosteroids for GVHD, chemotherapy for relapse, cytomegalovirus reactivation, and therapy), these parameters were determined only for the time post-transplant before these clinical events had transpired. ALCs after DLI were not considered as a part of this analysis.

T Cell Engraftment Analysis

Donor engraftment was measured using chimerism analyses performed at approximately 4, 8, 12, and 24 weeks after transplant on immunomagnetically separated granulocytes and total T cells as previously described [13]. Donor-derived $CD3^+$ T cell count (ddCD3) was calculated by multiplying the T cell chimerism (% recipient DNA, expressed as a fraction) with the absolute blood $CD3^+$ T cell count obtained simultaneously. The resulting absolute recipient-derived $CD3^+$ T cell count was then subtracted from the total absolute $CD3^+$ cell count to obtain a ddCD3. When available, the calculated ddCD3 values for the first 3 to 6 months were plotted over time for each patient as a polynomial (cubic) function of time ($y = ax^3 + bx^2 + cx + d$) using Microsoft Excel software (Microsoft Corporation, Redmond, WA). This was done with the assumption that the ddCD3 on day 0 of SCT will be zero. From the resulting polynomial equations for each patient, the differential equation describing the rate of change of ddCD3 at any time point along the curve for each patient was determined ($dy/dx = 3ax^2 + 2bx + c$). The derivative (ie, rate of change of ddCD3 at days 30 and 45)

was then calculated for each individual using Wolfram/Alpha Online Derivative Solver (Wolfram/Alpha LLC, Champaign, IL). These early points were chosen because they represented the earliest clinically important measured ddCD3 value available and because these allowed determination of the T cell expansion rate in the time period immediately after the cessation of MMF. The derivative calculations were also confirmed by manual calculations.

Study Design and Statistical Analysis

For this analysis overall survival was taken from the day after transplant to the day of death. GVHD was classified according to consensus criteria. Acute GVHD was graded according to the Glucksberg criteria. GVHD observations were censored if this complication developed after DLI. Disease-specific criteria were used for diagnosing relapse or progression. Survival and event-free survival curves (relapse-fatality) for the 5.1- and 7.5-level dose groups were plotted with Kaplan-Meier curves and compared using the log-rank test. The incidence curves for relapse, acute GVHD, chronic GVHD, and DLI use (accounting for the competing risk of mortality) were plotted and compared between dose levels using Grey's test. Wilcoxon rank sum tests were used to compare median percentage chimerism and ddCD3 cell count between dose groups at different times after SCT; this nonparametric test was used because these measures exhibit highly nonsymmetrical distributions. The R statistical software (version 2.15; Revolution Analytics, Mountain View, CA) was used for all time-to-event analyses, with the *survival* package used for survival curves and the *cmprsk* package used for all competing risk curves.

The rate of change in ddCD3 cell count at day 30 ($dx/dy(30)$) and day 45 ($dx/dy(45)$) after SCT was summarized with medians and interquartile ranges for each level (yes/no) of the following clinical outcomes: GVHD, relapse, survival, and DLI use. The Wilcoxon rank sum test was used to compare medians in $dx/dy(30)$ and $dx/dy(45)$ between the levels of those health outcomes and other variables studied. A 5% significance level was used for purposes of testing null hypotheses that these values are equal across the 2 levels of the clinical outcomes versus 2-sided alternative hypotheses. The Kruskal-Wallis test was used to compare monocyte count medians between lymphocyte recovery patterns. A 5% significance level was used for purposes of testing null hypotheses, and a Bonferroni-adjusted level of .1067 ws used in cases of multiple comparisons between logistic characteristic patterns. The NPAR1WAY procedure was used in the SAS statistical software (version 9.4; SAS Institute, Cary, NC) for all analyses. The Pearson correlation coefficient was used to measure the relationship between logistic growth patterns in lymphocyte recovery and $CD3^+$ dose, $CD34^+$ dose, and tacrolimus level area under the curve.

Results

Clinical Outcomes with ATG+TBI Conditioning

This study was designed to examine the relative impact of 2 ATG doses in a RIC regimen on immune reconstitution and subsequent clinical outcomes, with the aim of improving survival by limiting fatal GVHD while retaining GVM effects. At last follow-up there were no significant differences in the survival between the 2 study arms (log-rank $P = .53$) (Figure

1A). The 1- and 2-year survival rates in the ATG 5.1 cohort were both 71.3% (standard error [SE] = 1.1%), whereas those in the 7.5 cohort were 90.9% (SE = .4%) and 62.4% (SE = 1.2%), respectively.

The conditioning regimen was tolerated well with no day 100 transplant-related mortality observed. The treatment-related mortality rate and relapse rate were not significantly different between the 2 dose groups (Grey's test $P = .82$ and .62, respectively) (Figure 1B). The 1- and 2-year relapse rates in the ATG 5.1 cohort were 21.8% (SE = .8%) and 28.0% (SE = 1.1%), respectively, and in the ATG 7.5 cohort were 40.9% (SE = 1.2%) and 50.0% (SE = 1.2%), respectively. Event-free survival was also comparable between the 2 arms ($P = .76$) (Figure 1C).

Accounting for the competing risk of mortality, acute GVHD rate in the ATG 5.1 cohort was 27.2% (SE = 1.0%) and in the 7.5 dose group 4.5% (SE = .2%) ($P = .039$) (see Supplemental Material for details). Similarly, accounting for the competing hazard of mortality, the 1- and 2-year chronic GVHD rates in the ATG 5.1 cohort were both 23.8% (SE = .94%) and in the ATG 7.5 group 31.8% (SE = 1.1%) and 36.8% (SE = 1.2%), respectively ($P = .37$) (Figure 1D).

The need for post-transplant cellular therapy intervention, DLI (administered for either mixed chimerism or persistent disease or relapse) was greater in the ATG 7.5 arm. Accounting for the competing risk of mortality, the 1- and 2-year DLI rates in the ATG 5.1 arm were both 8.9% (SE = .4%), whereas in the ATG 7.5 arm it was 40.9% (SE = 1.1%) and 45.5% (SE = 1.2%), respectively (Grey's test $P = .072$) (Figure 1E).

Engraftment

To determine the dose effect of ATG on T cell and myeloid engraftment in this RIC regimen, T cell chimerism and absolute T cell count recovery and granulocyte chimerism were compared between the 2 arms. T cell chimerism was mixed donor–recipient in a number of patients, with a larger recipient-derived component in the ATG 7.5 cohort compared with the ATG 5.1 cohort, except at 9 months (where both medians were 0) (Table 2). Correspondingly, the ddCD3 cell counts were higher in the ATG 5.1 cohort than in the ATG 7.5 cohort at every time point (Supplemental Figure 2, Table 2). Myeloid engraftment was donor derived in all but 3 patients in the ATG 7.5 cohort. These results demonstrate that hematopoietic engraftment was superior in the ATG 5.1 cohort.

Lymphoid Reconstitution Kinetics

To study the influence of the rate ofimmunereconstitution on clinical outcomes in individual patients, ALCs (μL^{-1}) for each individual were plotted over time to model immune reconstitution kinetics. Similar to population growth models, lymphocyte recovery after SCT occurred as a logistic function of time. In a number of patients, 2 discernable periods of exponential increase in ALC were observed, 1 after engraftment and another period after cessation of MMF (Figure 2A, Supplemental Figure 3). These growth periods were each followed by a plateau, representing the steady state immune cell recovery at that phase of SCT, with relatively stable lymphocyte counts in the absence of clinical events until withdrawal of tacrolimus, when greater variability was observed, and a trend of a further

increase in ALC was frequently observed. On examination of individual lymphocyte recovery plots, 3 general patterns of lymphoid recovery were observed over time (Figure 2B): pattern A (n = 15), sigmoid growth with early, rapid lymphoid expansion and a high steady state level (ALC > 1000 μL^{-1}, inflection point <60 days post-SCT); pattern B (n = 14), a lower steady state level arrived at slowly (ALC ≥ 500 to 1000 μL^{-1}, inflection point > 60 days); and pattern C (n = 10), poor ALC recovery with minimal to no discernable sigmoid growth kinetics (ALC <500 μL^{-1}). Two patients from the ATG 7.5 cohort with good lymphoid recovery (pattern A) but predominantly recipient T cell chimerism were excluded from this analysis. Patients developing complications of therapy such as relapse, viral reactivation (cytomegalovirus or Epstein-Barr virus), and GVHD requiring corticosteroid therapy had significant departures from the sigmoidal curve generally after reaching a plateau (Supplemental Figure 3). Logistic curve fitting patients with pattern A demonstrated the double exponential expansion periods (median R^2, .90 and .89, respectively, n = 15), with median growth exponent(R in the logistic equation) values of .94 and .18 for the 2 periods, respectively. Pattern B patients similarly demonstrated logistic growth (median R^2, .83, n = 14), albeit with a much slower growth rate of .04.

Logistic patterning was significantly associated with all clinical outcomes, including survival in 67% versus 86% versus 30% of patients in pattern A, B, and C groups, respectively (exact test P value = .0189); relapse in 33%, 29%, and 90% (P = .0053); cumulative GVHD in 67%, 43%, and 10% (P = .0198); and DLI use in 13%, 21%, and 70% of patients, respectively (P = .0069). Pattern C patients had a particularly poor outcome in terms of survival, relapse, and need for DLI.

Determinants of Logistic Patterning

To identify factors influencing logistic growth patterns observed in lymphocyte recovery (ATG dose, donor type and age, diagnosis, prior therapy, $CD3^+$ and $CD34^+$ cell doses infused), tacrolimus level area under the curve for days 15, 30, and 60 were reviewed and did not demonstrate statistically significant association with the ALC curve logistic patterns recorded. Reasoning that the lymphocyte growth exponent, R, for T cells will be influenced by antigen presentation before the period of exponential growth, the monocyte recovery curves after SCT were plotted for each individual and overlaid with the T cell expansion curve. After engraftment, there was correspondence in the lymphocyte and monocyte growth curves, both demonstrating logistic dynamics (Figure 3A, Supplemental Figure 4). Furthermore, there was a strong association between the maximal circulating monocyte counts (μL^{-1}) recorded between days 12 and 16 (periengraftment) and the logistic patterns observed in lymphocyte recovery over the first 3 months post-transplant; these values were 600, 350, and 200, respectively, in patients with lymphocyte recovery patterns A, B, and C (P = .0002). Robust monocyte recovery post-engraftment may be associated with greater likelihood of recipient (and microbial) antigen presentation in the earliest days after SCT, yielding higher values of R and faster lymphocyte expansion.

Donor-Derived T Cell Recovery Kinetics

To identify the cell subset associated with lymphoid expansion and to determine the effect of donor-derived T cell recovery kinetics on clinical outcomes, the ddCD3 counts were plotted

as a function of time for the first 6 months after SCT for patients for whom data were available. Using the equation for the resulting curves, the derivative equation of each curve was then calculated to allow the determination of an approximate, instantaneous rate of change of ddCD3 at various times along the plotted curve (Figure 3B). The derivative of this curve for each patient dx/dy was calculated for days 30 and 45 post-SCT to assess the impact of early T cell reconstitution on clinical outcomes. The dx/dy values obtained in this ATG conditioned set of patients for days 30 and 45 were highly correlated with each other (Spearman's correlation coefficient, $R^2 = .91$). They also correlated with the logistic patterns of ALC recovery observed in each patient, suggesting the exponential expansion observed in the ALC may be due to ddCD3 proliferation. Both the $dx/dy(30)$ and $dx/dy(45)$ medians were significantly different between logistic classifications (Table 3); specifically, patients with pattern A logistic lymphoid recovery had higher $dx/dy(30)$ compared with those demonstrating both pattern B ($P = .0014$) and pattern C ($P \leq .001$). For $dx/dy(45)$, pattern C patients had significantly lower levels than both pattern A ($P = .0063$) and pattern B patients ($P = .0063$) (using Bonferroni-adjusted significance level of .0167). This suggests the exponential expansion observed in the lymphocyte recovery patterns was attributable to ddCD3 proliferation. And even though *instantaneous* measures of ddCD3 cell expansion, the day 30 and 45 ddCD3 derivative measurements generally correlated with clinical outcomes (Table 4). This measure at day 30 was significantly different between patients experiencing GVHD ($P = .0026$) and those requiring DLI ($P = .0476$), indicating the influence of early donor T cell expansion on alloreactivity.

Discussion

Patients undergoing HLA matched allogeneic SCT are at risk for competing hazards of relapse, nonrelapse mortality, and alloreactivity (ie, GVHD or graft rejection), potentially leading to treatment failure [32]. Beyond tumor biology, the 2 most critical factors influencing treatment failure are regimen-related toxicity of the SCT and T cell reconstitution after transplantation, with its effects on alloreactivity and opportunistic infections. Once regimen-related toxicity is diminished using RIC regimens, the ability to forecast and manage the restoration of T cell immunity would be of great value in terms of optimizing clinical outcomes. In this study we found that T cell reconstitution after SCT is a dynamic process that can be modeled by equations commonly used to describe growth in biological systems. Furthermore, the dynamics of T cell reconstitution have a major impact on important clinical outcomes such as GVHD and engraftment as well as survival. This suggests that the likelihood of certain clinical outcomes may be computed in real time during the course of SCT and appropriate therapeutic adjustments made dynamically, rather than at specific time points post-transplant.

Systems following logistic dynamics, modeling constrained growth, depicted by the sigmoid curve, are common in biology [22,23], describing phenomenon as diverse as population growth (in both the microbial and in the animal kingdom) and enzyme reaction kinetics with saturation. The hypothesis that they should also describe lymphocyte reconstitution after an immunoablative SCT is rational and supported by our data. Further support for this concept comes from the observation that, as expected, clinical events such as GVHD and infections and relapse lead to a departure from steady state behavior evident in these curves. An

important consideration in reviewing the ALC data presented here is that many different immune cell subsets constitute these curves, natural killer cells, T cell subsets, and B cells, with all the cell subsets following different growth kinetics; therefore, the ALC growth curves seen here are an average of all those influences. Correlation of these growth curves with donor-derived T cell counts, however, makes it evident that this constitutes the dominant immune cell population leading to the *late exponential growth* (after cessation of MMF in the second month after SCT with this regimen) and its subsequent influence on long-term clinical outcome, whether it be GVHD after withdrawal of immunosuppression or long-term disease control. Once again supporting this idea is the observation of eventual relapse and DLI need in patients who did not experience this late lymphoid/ddCD3 cell expansion.

There are important clinical implications of this dynamical system modeling of SCT, the most important is that it identifies subgroups of patients at greater risk for certain transplant outcomes over others (relapse or GVHD), increasing the predictability of the clinical course likely to be observed in individual SCT recipients. For instance, patients with logistic pattern A, or with a high rate of change of ddCD3 at day 30 in our 2 cohorts, were more likely to develop late onset acute or chronic GVHD when immunosuppression was withdrawn. Patients with logistic pattern C were more likely to require DLI or to relapse. This behavior suggests that plotting ALC and/or ddCD3 in the first few weeks after SCT may allow categorization of patients into risk groups based on dynamic immune reconstitution. Future interventions may then be planned accordingly. This may include prolonged immunosuppression with tacrolimus in those with high derivative ddCD3 values or closer monitoring and preemptive therapy for cancer relapse in those with lower values.

Certain dynamical systems demonstrate strong influence of early conditions on late outcomes. To understand this, consider an idealized situation where the natural killer cell and B cell effect on clinical outcome is negligible and clinical outcomes, such as GVHD, GVM (considering standard risk malignancy in a minimal residual disease state), and engraftment, are a function of T cell reconstitution. Here, the T cell population, N_{t+1}, at time, $t+1$ after SCT, is a function of the T cell population N_t, at an earlier time point, t. This in turn will be dependent on the T cell population at the outset of transplant N_0 and the growth rate R governing the growth, such that

$$N_0 \xrightarrow{[\mathrm{R}]} N_t \xrightarrow{[\mathrm{R}]} N_{t+1} \xrightarrow{[\mathrm{R}]} K$$

In this model (Figure 4) the final steady state population of T cells, K, and its clonal repertoire will have a major influence on clinical outcomes. An approximation of this growth rate for donor-derived T cells at various times after SCT is provided by the derivative we calculated. In this model initial conditions (ie, N_0 and R) impact the trajectory of lymphoid recovery after SCT. The higher rate of mixed T cell chimerism and lower ddCD3 cell count observed several months after the transplant in the ATG 7.5 cohort is consistent with this initial effect. Although the population differences in clinical outcomes are not statistically significant between the 2 cohorts, it is noteworthy that an ATG dose difference

of 2.4 mg/kg may have an influence on immune reconstitution and subsequent clinical outcomes, reflected by absence of late acute GVHD and a greater need for DLI, as well as graft loss in 3 individuals conditioned with the higher ATG dose. Presumably, this results from a higher ATG level at the time of cell infusion, leading to lower in vivo N_0 and also potentially a lower value of R in these patients.

To understand the cellular basis of the relationship between immune cell reconstitution kinetics and clinical outcomes (GVHD, relapse), it is important to recognize that the ALC curves we obtained, as well as the ddCD3 curves, represent an average measure of the proliferation of thousands of different T cell clones, when defined by T cell receptor specificity. These T cell clones are expected to follow growth curves similar to this average growth curve recorded in each individual but with different parameters. Further, the expansion of ddCD3 cells would be in part dependent on antigen presentation, with T cell clones presented with antigen more likely to proliferate rapidly. Thus, in patients with more robust hematopoietic recovery, it is likely that the average value of R would be greater because antigen presenting cell populations reconstitute faster. Considering monocytes as a surrogate for antigen presenting cells, the correspondence of early monocyte recovery with lymphoid recovery patterns observed supports this hypothesis. In fact, this may represent an example of *interacting dynamical systems*, where the R value in one drives the same in the other system. Thus, the $R_{antigen\ presenting\ cell}$ value may drive the $R_{effector\ T\ cell}$ by altering the cytokine concentrations in the post-transplant milieu, with ambient immunosuppression impacting both systems. The quantitative immune reconstitution model described here is well known, with the familiar sigmoid growth kinetics of lymphocytes and by extension T cell subsets and natural killer cells and the salutary effect of early lymphoid recovery on clinical outcomes after SCT [15,33]. The novelty of this work is in that it formalizes the understanding of the nature of immune recovery post-transplant as a dynamical system by clearly demonstrating an exponential expansion of lymphocytes, which occurs at variable rates.

This dynamical system modeling differs from stochastic modeling of transplant outcomes in individuals because it allows associations between immune reconstitution kinetics and clinical endpoints (either freedom from GVHD or not). In practice this would imply that immune cell subsets are measured frequently in the first few weeks after transplantation in each SCT recipient. Rate of lymphoid reconstitution at different times after SCT may then allow an estimation of the likelihood of alloreactivity developing in that specific patient and the corresponding clinical outcome. The probability of the desired outcome, P at time $t+1$, is dependenton all states of the system leading upto the time t, preceding $t+1$; as explained above, the trajectory of the system. This way clinical outcomes may be projected based on the lymphocyte recovery kinetics observed in the first few weeks after SCT. On the other hand, in a stochastic model the probability P of the desired outcome at time $t+1$ is a function of the probability distribution of the health state observed at time t and is unaffected by states of the system leading up to that time [34]. Therefore, an important advantage of dynamical system modeling is that by active measurement and intervention, this allows therapies to be modified on an ongoing basis to achieve desired clinical outcomes. On the other hand, conventional stochastic modeling allows selection of the optimal therapeutic program, but once the treatment is initiated it can only predict the outcomes observed based

on prior probability distributions, allowing only empiric therapeutic modifications. Dynamical system modeling of immune reconstitution would allow true personalization of patient management. Thus, patients with the logistic pattern A would be more likely to have had rapid oligoclonal expansion of alloreactive T cell clones and may be best managed with a prolonged course of immunosuppression to diminish the likelihood of delayed onset acute GVHD or severe chronic GVHD [35]. Conversely, patients with pattern C with limited T cell clonal recovery may benefit from early withdrawal of immunosuppression and DLI, before conventional time points such as days 100 or 180 post-transplant, to establish GVM effects before progression of malignancy, especially in the context of RIC. These patients may also benefit from disease-specific post-transplant therapies instituted along with planned DLI to prevent early relapse. Patients with pattern B would be the most likely to avoid life-threatening GVHD and have GVM develop given the slower but more complete lymphoid reconstitution with greater T cell clonal diversity. Next generation sequencing techniques such as high-throughput sequencing of T cell receptor β considered along with quantitative T cell reconstitution data discussed in this article will help further define therapeutic needs. Integrating information about tumor growth kinetics and donor recipient minor histocompatibility antigen differences will further help individualize therapeutic decision-making in the aftermath of SCT.

In conclusion, we demonstrate that immune reconstitution after SCT may be modeled mathematically using equations commonly used to describe population growth. Immune reconstitution after other conditioning and GVHD prophylaxis regimens will in all likelihood follow the same logistic dynamics but with different growth parameters. Therefore, further study of quantitative T cell repertoire reconstitution will allow determination of the degree to which such measurement may be generalizable and as such allow real time adjustments to be made in post-transplant immunosuppression, resulting in optimal immunosuppression. Importantly, dynamical system modeling of transplant makes it possible to limit the effect of randomness in predicting clinical outcomes such as GVHD and engraftment and further refine trial design by accounting for immune reconstitution kinetics.

Supplementary Material

Refer to Web version on PubMed Central for supplementary material.

Acknowledgments

The authors gratefully acknowledge Ms. Carol Cole, Laura Couch, Judith Davis, Angela Buskey, Dana Broadway, and Kathryn Candler for their excellent help in executing this protocol and the care of the patients enrolled on this study. We also acknowledge the Virginia Commonwealth University BMT program's nurse practitioners and nurses for their contributions towards the completion of this study.

References

1. Alousi AM, Le-Rademacher J, Saliba RM, et al. Who is the better donor for older hematopoietic transplant recipients: an older-aged sibling or a young, matched unrelated volunteer? Blood. 2013; 121:2567–2573. [PubMed: 23361908]
2. Woolfrey A, Lee SJ, Gooley TA, et al. HLA-allele matched unrelated donors compared to HLA-matched sibling donors: role of cell source and disease risk category. Biol Blood Marrow Transplant. 2010; 16:1382–1387. [PubMed: 20447462]

3. Saber W, Opie S, Rizzo JD, et al. Outcomes after matched unrelated donor versus identical sibling hematopoietic cell transplantation in adults with acute myelogenous leukemia. Blood. 2012; 119:3908–3916. [PubMed: 22327226]

4. Devillier R, Fürst S, El-Cheikh J, et al. Antithymocyte globulin in reduced-intensity conditioning regimen allows a high disease-free survival exempt of long-term chronic graft-versus-host disease. Biol Blood Marrow Transplant. 2014; 20:370–374. [PubMed: 24315846]

5. Nagler A, Rocha V, Labopin M, et al. Allogeneic hematopoietic stem-cell transplantation for acute myeloid leukemia in remission: comparison of intravenous busulfan plus cyclophosphamide (Cy) versus total-body irradiation plus Cy as conditioning regimen–a report from the acute leukemia working party of the European group for blood and marrow transplantation. J Clin Oncol. 2013; 31:3549–3556. [PubMed: 23980086]

6. Bredeson C, LeRademacher J, Kato K, et al. Prospective cohort study comparing intravenous busulfan to total body irradiation in hematopoietic cell transplantation. Blood. 2013; 122:3871–3878. [PubMed: 24081656]

7. Birnbaum A. On the foundations of statistical inference. J Am Stat Assoc. 1962; 298:269.

8. Klein, JP. Statistical analysis in hematopoietic stem cell transplantation. In: Atkinson, K.; Champlin, R.; Ritz, J., et al., editors. Clinical bone marrow and blood stem cell transplantation. 3rd. NewYork: Cambridge University Press; 2004. p. 1695

9. Duléry R, Mohty M, Duhamel A, et al. Antithymocyte globulin before allogeneic stem cell transplantation for progressive myelodysplastic syndrome: a study from the French Society of Bone Marrow Transplantation and Cellular Therapy. Biol Blood Marrow Transplant. 2014; 20:646–654. [PubMed: 24462982]

10. Reshef R, Hexner EO, Loren AW, et al. Early donor chimerism levels predict relapse and survival after allogeneic stem cell transplantation with reduced-intensity conditioning. Biol Blood Marrow Transplant. 2014; 20:1758–1766. [PubMed: 25016197]

11. Nash RA, Storb R. Graft-versus-host effect after allogeneic hematopoietic stem cell transplantation: GVHD and GVL. Curr Opin Immunol. 1996; 8:674–680. [PubMed: 8902393]

12. Horowitz MM, Gale RP, Sondel PM, et al. Graft-versus-leukemia reactions after bone marrow transplantation. Blood. 1990; 75:555–562. [PubMed: 2297567]

13. Toor AA, Sabo RT, Chung HM, et al. Favorable outcomes in patients with high donor-derived t cell count after in vivo t cell-depleted reduced-intensity allogeneic stem cell transplantation. Biol Blood Marrow Transplant. 2012; 18:794–804. [PubMed: 22005648]

14. Laurin D, Hannani D, Pernollet M, et al. Immunomonitoring of graft-versus-host minor histocompatibility antigen correlates with graft-versus-host disease and absence of relapse after graft. Transfusion. 2010; 50:418–428. [PubMed: 19843288]

15. Klyuchnikov E, Asenova S, Kern W, et al. Post-transplant immune reconstitution after unrelated allogeneic stem cell transplant in patients with acute myeloid leukemia. Leuk Lymph. 2010; 51:1450–1463.

16. Berger M, Figari O, Bruno B, et al. Lymphocyte subsets recovery following allogeneic bone marrow transplantation (BMT): $CD4^+$ cell count and transplant-related mortality. Bone Marrow Transplant. 2008; 41:55–62. [PubMed: 17934532]

17. Spierings E, Kim YH, Hendriks M, et al. Multicenter analyses demonstrate significant clinical effects of minor histocompatibility antigens on GvHD and GvL after HLA-matched related and unrelated hematopoietic stem cell transplantation. Biol Blood Marrow Transplant. 2013; 19:1244–1253. [PubMed: 23756210]

18. Miklos DB, Kim HT, Miller KH, et al. Antibody responses to H-Y minor histocompatibility antigens correlate with chronic graft-versus-host disease and disease remission. Blood. 2005; 105:2973–2978. [PubMed: 15613541]

19. Sampson JK, Sheth NU, Koparde VN, et al. Whole exome sequencing to estimate alloreactivity potential between donors and recipients in stem cell transplantation. Br J Haematol. 2014; 166:566–570. [PubMed: 24749631]

20. Jameson-Lee M, Koparde VN, Griffith P, et al. *In silico* derivation of HLA-specific alloreactivity potential from whole exome sequencing of stem cell transplant donors and recipients:

understanding the quantitative immunobiology of allogeneic transplantation. Frontiers Immunol. 2014; 5:529.

21. Meier J, Roberts C, Avent K, et al. Fractal organization of the human T cell repertoire in health and following stem cell transplantation. Biol Blood Marrow Transplant. 2013; 19:366–377. [PubMed: 23313705]
22. May RM. Biological populations with nonoverlapping generations: stable points, stable cycles, and chaos. Science. 1974; 186:645–647. [PubMed: 4412202]
23. May RM. Simple mathematical models with very complicated dynamics. Nature. 1976; 261:459–467. [PubMed: 934280]
24. Stewart, I. In pursuit of the unknown, 17 equations that changed the world. Philadelphia, PA: Basic Books; 2012. The imbalance of nature chaos theory; p. 283
25. Morrison, F. The art of modeling dynamic systems: forecasting for chaos, randomness and determinism. Mineola, NY: Dover Publications; 2008. A classification scheme for dynamic systems; p. 165
26. Toor AA, Kobulnicky JD, Salman S, et al. Stem cell transplantation as a dynamical system: are clinical outcomes deterministic? Frontiers Immunol. 2014; 5:613.
27. Luznik L, O'Donnell PV, Symons HJ, et al. HLA-haploidentical bone marrow transplantation for hematologic malignancies using non-myeloablative conditioning and high-dose, post-transplantation cyclophosphamide. Biol Blood Marrow Transplant. 2008; 14:641–650. [PubMed: 18489989]
28. Koreth J, Stevenson KE, Kim HT, et al. Bortezomib-based graft-versus-host disease prophylaxis in HLA-mismatched unrelated donor transplantation. J Clin Oncol. 2012; 30:3202–3208. [PubMed: 22869883]
29. Portier DA, Sabo RT, Roberts CH, et al. Anti-thymocyte globulin for conditioning in matched unrelated donor hematopoietic cell transplantation provides comparable outcomes to matched related donor recipients. Bone Marrow Transplant. 2012; 47:1513–1519. [PubMed: 22580767]
30. Barrett J. Improving outcome of allogeneic stem cell transplantation by immunomodulation of the early post-transplant environment. Curr Opin Immunol. 2006; 18:592–598. [PubMed: 16872820]
31. Savani BN, Mielke S, Rezvani K, et al. Absolute lymphocyte count on day 30 is a surrogate for robust hematopoietic recovery and strongly predicts outcome after T cell-depleted allogeneic stem cell transplantation. Biol Blood Marrow Transplant. 2007; 13:1216–1223. [PubMed: 17889359]
32. Kim HT. Cumulative incidence in competing risks data and competing risks regression analysis. Clin Cancer Res. 2007; 13(2 Pt 1):559–565. [PubMed: 17255278]
33. Bartelink IH, Belitser SV, Knibbe CA, et al. Immune reconstitution kinetics as an early predictor for mortality using various hematopoietic stem cell sources in children. Biol Blood Marrow Transplant. 2013; 19:305–313. [PubMed: 23092812]
34. Morrison, F. The art of modeling dynamic systems: forecasting for chaos, randomness and determinism. Mineola, NY: Dover Publications; 2008. Stochastic systems–type IV; p. 278
35. Berrie JL, Kmieciak M, Sabo RT, et al. Distinct oligoclonal T cells are associated with graft versus host disease after stem-cell transplantation. Transplantation. 2012; 93:949–957. [PubMed: 22377792]

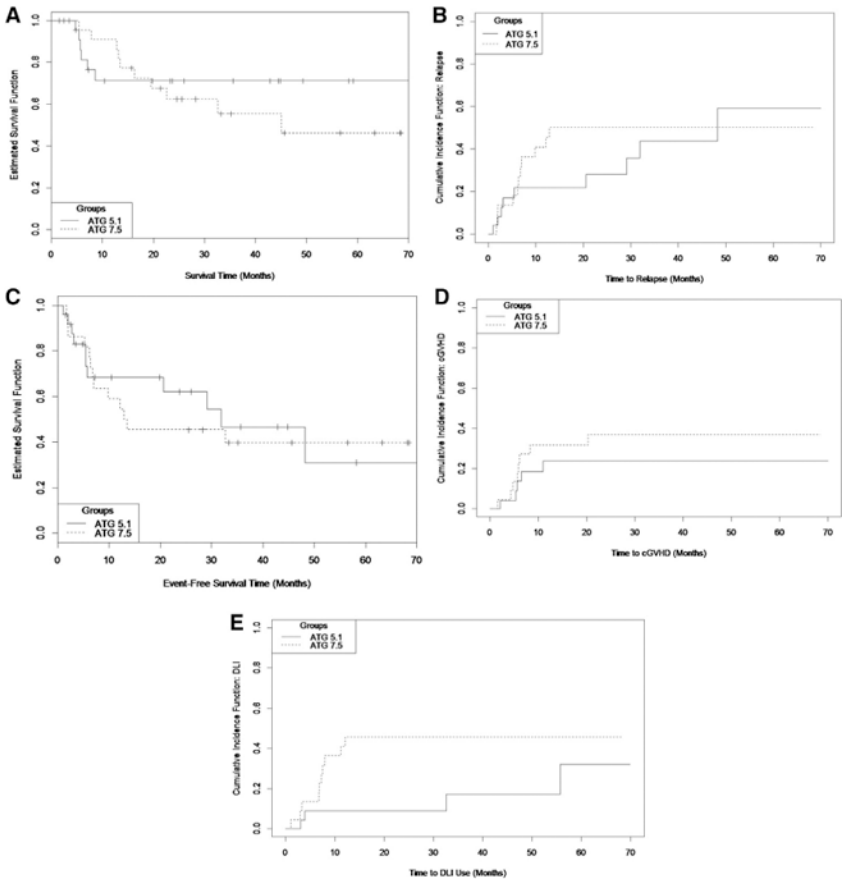

Figure 1.

Clinical outcomes in the ATG 5.1 and ATG 7.5 cohorts. (A) Kaplan-Meier survival curves. (B) Cumulative incidence curves for relapse (competing risk of transplant-related mortality). (C) Kaplan-Meier event-free survival (relapse and fatality). (D) Cumulative incidence curves for chronic GVHD, observations censored at DLI (competing risk of fatality without GVHD). (E) Cumulative incidence curve for DLI (competing risk of fatality).

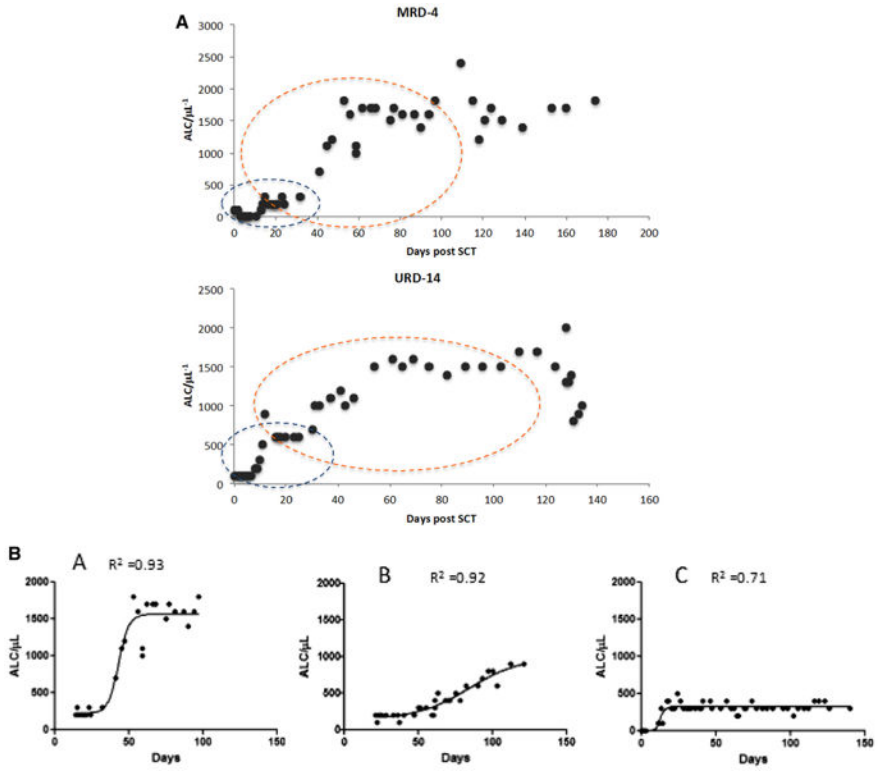

Figure 2.

ALC (μL^{-1}) recovery after ATG+TBI and SCT. (A) Two periods of growth are seen, first from days 0 to 30 when patients are on MMF (blue outline) and the second from day 20 to approximately day 120 (orange outline). Each period demonstrates an initial phase of slow growth, followed by exponential expansion and finally relatively stable counts, until tacrolimus is discontinued, when greater variability is observed. Data from a matched related donor (MRD) and an unrelated donor (URD) SCT are shown. (B) Logistic dynamics of lymphoid recovery after SCT. Three patterns are observed corresponding to high, pattern A; intermediate, pattern B; and slow growth rate, pattern C.

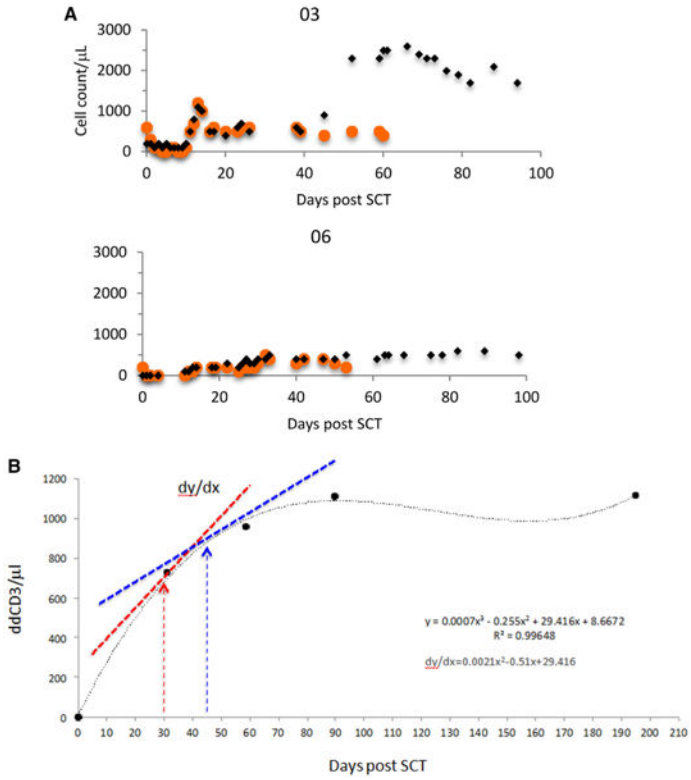

Figure 3.

Determinants of lymphoid recovery. (A) Correspondence of early monocyte recovery with lymphocyte reconstitution, association of high early monocyte recovery with late lymphoid expansion (orange circles indicate monocytes; black diamonds, lymphocytes) plotted against days post-SCT. (B) ddCD3 cell count plotted over time, and derivative for the polynomial curve determined at days 30 and 45. Derivative is the slope of the tangent to the polynomial curve (dy/dx) and gives the approximate rate of change of ddCD3 at that point in time. Accuracy of the derivative depends on the goodness of fit of the polynomial curve.

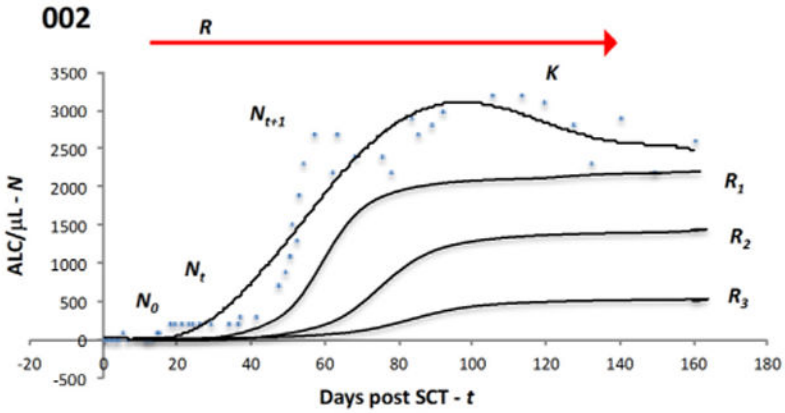

Figure 4.

Logistic model of lymphocyte proliferation post-transplant. Cell dose infused at the time of SCT N_0 will start proliferating under the influence of the driving parameter R and expand over time t, taking on values of N_t, N_{t+1},., N_{t+n}. This will include a period of exponential expansion as the lymphopenic state after SCT is corrected and eventually a stable lymphocyte population K is established. Changes in antigen presentation (due to infection, tissue injury) and immunosuppression levels and the overall cytokine milieu may perturb the steady state or growing populations by altering R and result in greater variability seen at specific time points. Reconstitution of the lymphocyte subset populations by differentiation of hematopoietic cells also changes N. The curves represents an average of the lymphoid cell populations (and clones) seen in circulation, with each population repopulating with similar dynamics but at different rates. Three other hypothetical curves along the continuum of logistic expansion are also shown with different N_0 (not evident due to scale) and R values ($R > R1 > R2 > R3$). Blue circles and top curve depict data from an actual patient.

Table 1

Patient Characteristics

	ATG 5.1	ATG 7.5
N	19	22
Male	12	14
Median age (range)	57 (44-69)	57 (40-68)
Donor		
Matched related donor	9	10
Unrelated donor	10	12
HLA Mismatch	2	2
Stem cell source		
Bone marrow	2	2
Peripheral blood	17	20
Diagnosis and prior therapy		
MM	5	4
NHL	7	8
AML	1	3
MDS	0	2
CLL	4	3
PLL	2	2
Median no. of prior regimens (range)	4 (2-10)	4 (1-15)
Prior autologous SCT	6	8
Median cell dose infused		
$CD3^+ \times 10^6$/kg (range)	2.3 (.1-5.7)	2.9 (.2-11.3)
$CD34^+ \times 10^8$/kg (range)	5.8 (1.7-10.4)	5.1 (1.6-7.5)

MM indicates multiple myeloma; NHL, non-Hodgkin lymphoma; AML, acute myelogenous leukemia; MDS, myelodysplastic syndrome; CLL, chronic lymphocytic leukemia; PLL, prolymphocytic leukemia.

Table 2

Median Percentage Recipient Chimerism (Top) and ddCD3 Cell Counts (Bottom) by ATG Dosing Cohort and Time Post-SCT

	Time Post-SCT					
	1 mo	**2 mo**	**3 mo**	**6 mo**	**9 mo**	**12 mo**
ATG 7.5	6.7	8.8	18.5	8.7	.0	1.4
ATG 5.1	.0	1.0	1.5	.0	.0	.0
P on differences	.20	.16	.024*	.056	.052	.077
ATG 7.5	93.3	105.8	92.1	225.7	352.0	493.0
ATG 5.1	214.1	576.6	405.0	408.0	853.7	680.0
P on differences	.068	.073	.031*	.63	.071	.18

*Statistically significant at $P<.05$.

Table 3

Correlation of Rate of Change in ddCD3 Cell Counts at Days 30 and 45 with ALC Recovery Logistic Patterns

Logistic pattern	*dx*/*dy*(30) ddCD3			*dx*/*dy* (45) ddCD3		
	n	Median	IQR	n	Median	IQR
A	14	15.5	12.2, 25.2	14	10.8	1.4, 17.3
B	14	2.5	.4, 3.9	14	1.5	.6, 26
C	5	.2	−.1,.5	5	.1	−.1, .5
	$P < .0001$			$P = .0015$		

Table 4

Correlation of Day 30 and Day 45 ddCD3 Derivative Values and Clinical Outcome on Patients in whom Data was Available to Allow Plotting of the Polynomial Curve

	Yes			No			*P*
	n	Median	IQR	n	Median	IQR	
dx/*dy*(30)							
GVHD	16	14.5	4.4, 16.5	17	.9	.1, 5.5	.0026
Relapse	14	2.3	−.1, 10.9	19	4.7	2.1, 16.0	.0869
Survival	22	4.5	.9, 15.6	11	3.7	.3, 15.5	.8635
DLI use	9	.9	.1, 5.2	24	7.1	1.4, 16.5	.0476
dx/*dy*(45)							
GVHD	16	3.4	1.2, 13.5	17	.7	.3, 2.3	.0562
Relapse	14	1.6	.4, 6.9	19	1.8	.9, 10.9	.4888
Survival	22	1.6	.8, 6.5	11	1.9	.1, 15.6	.9848
DLI use	9	.5	.3, 2.0	24	2.1	.9, 13.2	.1149